Open Access

OBM Transplantation

LIDSEN Publishing Inc.

Original Research

Systems Immunology of Colorectal Liver Metastases in the Context of Liver Transplantation: Multi-Omics Insights into Tumor Progression and Post-Transplant Recurrence

Elham Amjad [1, 2], Babak Sokouti [3, *]

1. Student Research Committee, Ahvaz Jundishapur University of Medical Sciences, Ahvaz, Iran; E-Mails: elham.amjad1996@gmail.com; amjad.e@ajums.ac.ir
2. Department of Medical Genetics, School of Medicine, Ahvaz Jundishapur University of Medical Sciences, Ahvaz, Iran
3. Biotechnology Research Center, Tabriz University of Medical Sciences, Tabriz, Iran; E-Mails: b.sokouti@gmail.com; sokoutib@tbzmed.ac.ir

* **Correspondence:** Babak Sokouti; E-Mails: b.sokouti@gmail.com; sokoutib@tbzmed.ac.ir

Academic Editor: Chirag S. Desai

Special Issue: Liver Transplantation for Colorectal Liver Metastases: Current Management and Future Perspectives

OBM Transplantation
2026, volume 10, issue 3
doi:10.21926/obm.transplant.2603276

Received: August 11, 2025
Accepted: September 01, 2026
Published: September 14, 2026

Abstract

After liver transplantation, colorectal cancer (CRC) recurrence is a serious clinical issue. This underscores the need to understand the molecular and immunometabolic axes that promote tumor development and transplant fragility. This research combines compound-gene network analysis, immune cell deconvolution, and transcriptome profiling to find important genes and pathways that connect post-transplant immune modulation and CRC development. ADH1B, ALB, and ZG16 are consistently altered in primary colorectal malignancies, metastatic liver lesions, and transplanted hepatic tissue. These genes are involved in ethanol and retinol metabolism, systemic inflammation, immune cell infiltration, and preservation of the mucosal barrier. Our research shows that these genes are at the center of a common immunometabolic axis that lets the body change its metabolism and evade the immune

system. Curcumin, beta-carotene, resveratrol, and D-mannitol are some of the bioactive dietary compounds that we find target these genes and related pathways. These could improve clinical outcomes in liver transplantation and colorectal cancer by changing how the immune system works. In addition to recommending ADH1B and ALB as potential biomarkers for recurrence monitoring and therapeutic targeting, this work offers a unified model of tumor-host-graft interactions. These findings lay the groundwork for future investigations that combine single-cell and spatial analysis to better understand gene function and direct precision therapies in transplant medicine and cancer, and are particularly relevant to patients undergoing liver transplantation for unresectable colorectal liver metastases (CRLM).

Keywords
Colorectal cancer; liver transplantation; immunometabolism; ADH1B; natural compounds

1. Introduction

Colorectal cancer (CRC) uses various immune evasion pathways, which have a significant impact on immunotherapy responses and clinical outcomes [1, 2]. One of the most noteworthy changes is an increase in immunological checkpoint proteins such as PD-1, PD-L1, and CTLA-4. These proteins inhibit T cells from activating, which allows malignancies to live and grow [1, 3, 4]. This is because a substantial proportion of individuals with dMMR CRC and high microsatellite instability (MSI-H) eventually develop primary or acquired resistance to immune checkpoint inhibitors [3]. This is due to the complex nature of the tumor microenvironment (TME), which includes suppressive cell types such as myeloid-derived suppressor cells (MDSCs) and regulatory T cells (Tregs) [3, 5]. The fact that mediators like IL-17 and TGF-β signaling worsen the breakdown of antitumor immunity and contribute to the poor prognosis further emphasizes the need for therapies that get around these barriers [6, 7]. To improve CRC outcomes, combinatorial strategies targeting both immunosuppressive factors and checkpoints may be required [5, 8].

Critical immunological checkpoints such as PD-1, PD-L1, and CTLA-4 play important roles in the progression of colorectal cancer (CRC) by creating an immunosuppressive tumor microenvironment (TME) and inhibiting T-cell responses [2, 9, 10]. Poor prognosis is connected to elevated PD-L1 expression on tumor cells [11], even though PD-1 suppression in MSI-H CRC is linked to increased T-cell proliferation, better survival, and therapeutic benefit [12, 13]. However, immune checkpoint inhibitors are less effective in microsatellite stable (MSS) or mismatch repair-proficient (pMMR) cancers. Lower levels of checkpoint expression and immune infiltration are the cause of this [14, 15]. Therefore, immune-targeted strategies have a lot of therapeutic potential, especially for immunologically active CRC subtypes [14, 15].

The risk of colorectal cancer recurrence is greatly increased after liver transplantation (LT) due to immunosuppression, which impairs antitumor immune surveillance. This is supported by evidence from transplant registries showing increased rates of de novo malignancies and recurrence of pre-existing cancers [16-20]. Calcineurin inhibitors such as tacrolimus have been associated with increased tumor recurrence after transplantation, whereas mTOR inhibitors (e.g., sirolimus, everolimus) have been investigated as potentially less oncogenic or even protective in selected

settings [21, 22]. However, the net effect of immunosuppressive regimens on CRC recurrence risk remains complex and regimen-dependent. Because of the relationship between immunosuppressive drugs and colorectal cancer development, it is critical to regularly monitor patients and identify alternative approaches to lower the risk of recurrence [23-25].

Little information is available on how LT-induced immunosuppression and CRC immune evasion interact. The effects of immunosuppressive drugs on the composition of the tumor microenvironment (TME), particularly MDSCs and immune checkpoints, and how they alter tumor aggressiveness, metastatic potential, and metabolic patterns are not well understood [26]. Additional obstacles to translational progress include data variability issues, a deficiency in multi-omics integration, a lack of longitudinal data, and insufficient patient diversity in the omics studies of CRC and transplantation that are currently available [27]. Systems immunology approaches in the setting of cancer recurrence after transplant are still in their infancy, although they are rare [28]. The multi-omics methodology that has helped with liver cancer subtyping and biomarker discovery may also help LT-CRC investigations [29, 30].

Liver transplantation has emerged as a promising curative option for carefully selected patients with unresectable colorectal liver metastases (CRLM) who have liver-only disease and favorable tumor biology [31-33]. However, post-transplant recurrence remains a major limitation due to lifelong immunosuppression. Understanding the molecular overlap between primary CRC, CRLM, and the post-transplant liver microenvironment is therefore critical for improving patient selection, surveillance, and adjuvant strategies in this specific population.

Therefore, this study aims to identify conserved immunometabolic axes that link colorectal cancer development, liver metastasis, and post-transplant recurrence using a systems immunology paradigm. By combining multi-omics analyses like transcriptomic profiling, immune cell deconvolution, and compound-gene interaction mapping, we hope to identify shared molecular signatures and propose biomarkers and therapeutic targets that may aid in liver transplant monitoring and cancer management.

2. Materials and Methods

The workflow of the analysis pipeline used in this study is shown in Figure 1.

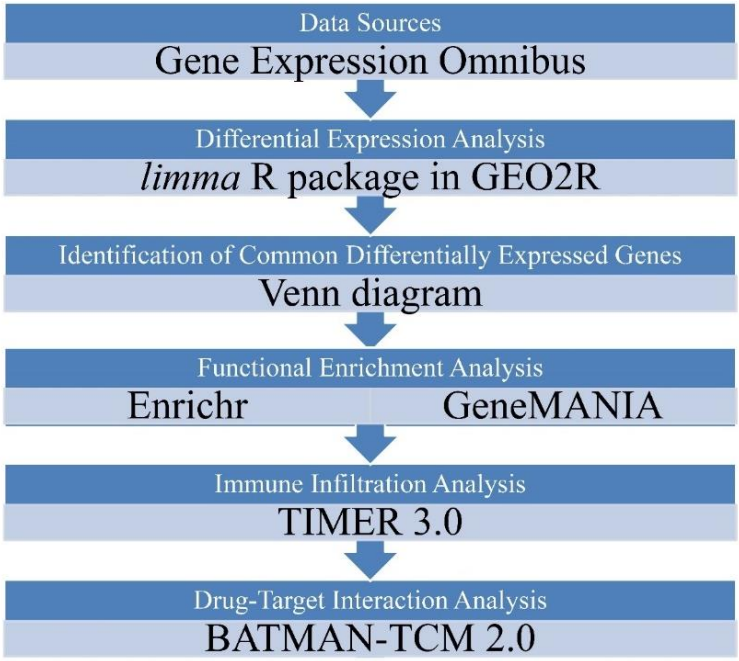

Figure 1 Workflow of the bioinformatics analysis pipeline. The study utilized data from the Gene Expression Omnibus (GEO), followed by differential expression analysis (limma R package in GEO2R). Common differentially expressed genes were identified and visualized via a Venn diagram. Functional enrichment was performed using Enrichr and GeneMANIA, while immune infiltration and drug-target interactions were analyzed with TIMER 3.0 and BATMAN-TCM 2.0, respectively.

2.1 Data Sources

We analyzed two transcriptomic datasets: GSE41258 and GSE14951. GSE41258 contains gene expression profiles from colorectal cancer (CRC) patients, including 186 primary colorectal tumor samples, 47 liver metastases (from CRC patients with hepatic metastatic disease), 54 matched normal colon tissues, and 13 normal liver samples. These liver metastases represent colorectal cancer-derived lesions in the liver, directly relevant to patients with colorectal liver metastases (CRLM). GSE14951 consists of five liver samples from patients after orthotopic liver transplantation and five healthy liver controls, providing insight into the post-transplant hepatic microenvironment.

2.2 Differential Expression Analysis

Differential gene expression analysis was performed using the GEO2R online interface, which implements the limma R package [34, 35]. The same standardized parameters were applied to all four comparisons: (1) liver metastases vs. primary tumors, (2) primary tumors vs. normal colon, (3) liver metastases vs. normal colon (GSE41258), and (4) liver transplant vs. normal liver (GSE14951). Genes were defined as differentially expressed (DEGs) if they satisfied $|\log_2 FC| > 1.5$ and adjusted p-value < 0.05, with p-values corrected for multiple testing using the Benjamini-Hochberg false

discovery rate (FDR) method [36]. Moderated t-statistics with empirical Bayes shrinkage were used to improve reliability with small sample sizes. Probe-to-gene mapping was performed using the latest Affymetrix annotation, selecting the probe with the highest interquartile range (IQR) in case of multiple probes per gene [37]. Quality control was assessed via boxplots of normalized intensities; no samples were excluded.

2.3 Identification of Common Differentially Expressed Genes

We identified genes that were consistently dysregulated across all experimental conditions by comparing the four lists of differentially expressed genes using the Multiple List Comparator tool (available at https://molbiotools.com/). Using this web-based platform, we compared gene lists from DEGs comparing primary tumors vs normal colon, liver metastases vs normal colon, liver metastases vs primary tumors, and liver transplant vs normal liver. To pass the analysis, genes must be present in all four comparisons and exhibit consistent directionality of expression change.

This study used Molbiotools' List Comparator tool because of its user-friendly design, ability to handle multiple gene lists at once, and clear visual output.

2.4 Functional Enrichment Analysis

Enrichr was used to functionally annotate the frequently differentially expressed genes using three Gene Ontology (GO) categories: Molecular Functions, Cellular Components, and Biological Processes [38]. Pathway analysis was performed using the Kyoto Encyclopedia of Genes and Genomes (KEGG) database [39]. The modified p-value criterion of less than 0.05 was utilized to determine statistical significance. Each phrase was required to include at least three genes, and broad terms with more than 500 genes in the background were discarded.

GeneMANIA was used to infer functional links based on co-expression, physical interactions, and shared protein domains using the protein-protein interaction analysis default settings [40, 41]. The GeneMANIA interface was used to visually display the results, with nodes from our differential expression analysis color-coded by expression directionality (blue for downregulated, red for upregulated).

2.5 Immune Infiltration Analysis

The immune cell composition of several sample groups was described using the most recent version of this computational deconvolution framework, TIMER 3.0 [42-44]. The research used the most current gene signatures for 64 distinct kinds of immune and stromal cells, as well as TIMER 3.0's upgraded xCell algorithm implementation. To process normalized gene expression matrices from all sample groups, we employed TIMER 3.0's $\log_2$ transformation and quantile normalization of input data, both of which are default choices. The platform's improved deconvolution accuracy, achieved by optimizing cell-type signature matrices using machine learning, enabled the provision of relative abundance estimates for key immune populations such as $CD8^+$ T cells, regulatory T cells, myeloid-derived suppressor cells, and macrophage subsets. TIMER 3.0 was used to perform statistical comparisons of immune infiltration levels among segments, with the built-in non-parametric testing module and Benjamini-Hochberg correction used.

2.6 Drug-Target Interaction Analysis

Potential therapeutic compounds targeting the common DEGs (particularly ADH1B and ALB) were identified using BATMAN-TCM 2.0 [45, 46]. We applied the following parameters: compound similarity score >0.5, FDR < 0.05, and at least three shared targets between compounds and query genes. Interactions were further filtered to include only those with published experimental evidence in the BATMAN-TCM database. Pathway proximity, sequence homology, and chemical structure similarity were integrated in the prediction algorithm.

2.7 Summary of Analytical Parameters

To enhance reproducibility, key parameters used across the bioinformatics pipeline are summarized as follows: Differential expression analysis in GEO2R/limma used $|\log_2 FC| > 1.5$ and Benjamini-Hochberg adjusted p-value < 0.05. Common DEGs were identified using consistent directionality across all four comparisons. We performed functional enrichment with Enrichr using adjusted p < 0.05 and a minimum of three genes per term. Immune infiltration analysis in TIMER 3.0 used default xCell signatures with Benjamini-Hochberg correction. BATMAN-TCM 2.0 predictions were filtered at similarity score >0.5, FDR < 0.05, and a minimum of three shared targets. All multiple testing corrections were performed using the Benjamini-Hochberg method unless otherwise specified.

3. Results

3.1 Identification of Conserved Differentially Expressed Genes

To determine whether genes were differentially expressed (DEGs) across the four groups under comparison, we used stringent criteria, including an adjusted p-value of less than 0.05 and an absolute $\log_2$ fold change greater than 1.5 ($|\log FC| > 1.5$). There were 1,962 differentially expressed genes (DEGs) in liver metastases compared to normal liver tissue (Liver Metastases (LM) vs. Normal Liver (NL)), 180 in liver metastases compared to primary tumors (LM vs. Primary Tumor (PT)), 1,526 in liver transplantation samples compared to normal liver (Liver Transplantation (LT) vs. NL), and 425 in normal colon tissue compared to primary tumors (Normal Colon (NC) vs. PT) among the numerous gene types identified in the study. The results demonstrate that the development of colorectal cancer, metastases, and the hepatic microenvironment after a transplant are all associated with significant alterations in the transcriptome. These alterations become more apparent when comparing the livers of individuals with and without liver metastases. The varying amounts of DEGs across comparison groups represent the distinct molecular landscape that each biological scenario has.

3.2 Differential Gene Expression Analysis Across GSE Datasets

We utilized GEO2R to discover differentially expressed genes (DEGs) across various conditions by evaluating publicly available datasets from the Gene Expression Omnibus (GEO). Volcano plots, expression distributions, sample annotations, and UMAP visualizations were used to examine expression profiles and sample clustering in each comparison (Figure 2).

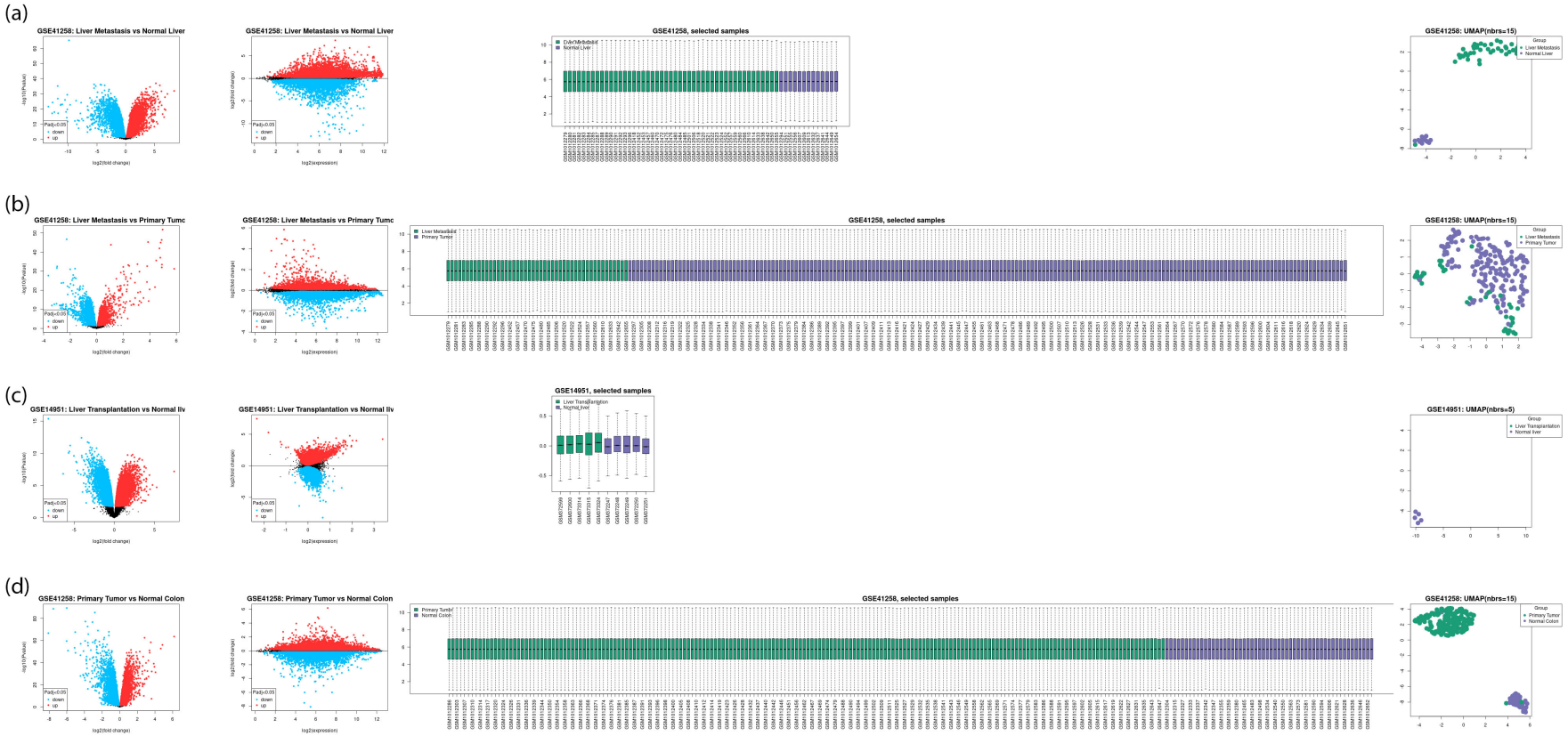

Figure 2 Differential gene expression analysis across multiple GEO datasets. (a) GSE41258: Liver metastasis vs. normal liver (1,962 DEGs). (b) GSE41258: Liver metastasis vs. primary tumor (180 DEGs). (c) GSE14951: Liver transplantation vs. normal liver (1,526 DEGs). (d) GSE41258: Primary tumor vs. normal colon (425 DEGs). Each panel displays (left to right): volcano plots of DEGs ($|\log_2 FC| > 1.5$, adjusted $p < 0.05$) with upregulated genes in red and downregulated genes in blue; expression distribution violin plots; sample annotation heatmaps; and UMAP plots showing sample clustering. UMAP plots demonstrate clear transcriptional separation between groups in panels (a), (c), and (d), while panel (b) shows partial overlap with distinct clustering trends between primary tumors and liver metastases, reflecting both shared and unique molecular features.

3.2.1 Liver Metastasis vs. Normal Liver (GSE41258)

A collection of differentially expressed genes (DEGs) was found in liver metastasis and normal liver tissue samples using a threshold of $|\log_2 FC| > 1.5$ and adjusted p-value < 0.05, as shown in the volcano plot on the left. A substantial number of genes were discovered to be either highly upregulated (red) or downregulated (blue). The violin plot (middle) depicts the distribution of log-expression values across groups and reveals similar expression ranges. The UMAP plot (right) shows a large grouping of liver metastasis and normal liver samples, indicating considerable transcriptome divergence, while the sample distribution heatmap (right center) confirms group separation.

3.2.2 Liver Metastasis vs. Primary Tumor (GSE41258)

Significant transcriptional differences between original colorectal cancers and liver metastases were shown by this comparison. There are many DEGs between the two groups, according to the volcano plot (left). The expression distribution plot (middle) shows similar gene expression dispersion. The grouped sample annotation heatmap verifies labeling and dataset integrity. The slightly overlapping but distinct clusters shown in the UMAP plot (right) represent both common and distinct transcriptome signatures across primary and metastatic locations.

3.2.3 Liver Transplantation vs. Normal Liver (GSE14951)

Comparing gene expression in normal liver tissues to transplanted liver samples resulted in a distinct DEG profile. The volcano image (left) demonstrates the significance of upregulation and downregulation patterns. The expression distributions (middle) demonstrate that gene expression differs across groups. The sample annotation boxplot, shown in the middle right, supports the uniformity of the sample labels. The clustering of the two groups, as shown by UMAP analysis (right), confirms their transcriptional separation.

3.2.4 Primary Tumor vs. Normal Colon (GSE41258)

To investigate tumor-specific changes in gene expression, primary colorectal tumor tissues were contrasted with normal colon tissue. The volcano plot shows a large number of DEGs (left). The median distribution of expression values indicates that the groups have a consistent expression range. Annotation heatmaps simplify sample categorization. The UMAP data, which are shown on the right, make it abundantly evident that the tumor and normal samples vary significantly biologically.

3.3 Functional Enrichment Analysis

Functional enrichment analysis using Enrichr revealed significant associations (adjusted p < 0.05) with Gene Ontology terms. In Biological Processes (2025), the top enriched terms included retinol metabolic process (GO:0042572), retinoic acid metabolic process (GO:0042573), and retinoid metabolic process (GO:0001523). Molecular Functions were enriched for dehydrogenase activities, including all-trans-retinol dehydrogenase (NAD+) activity (GO:0004745). Cellular Components showed enrichment for secretory elements such as Golgi lumen and collagen-containing extracellular matrix.

Cell type enrichment (CellMarker 2024) indicated strong association with goblet cells across multiple tissues (colon and small intestine, both human and mouse). Tissue-specific expression (GTEx v8 and Human Gene Atlas) was prominent in colon, liver, fetal liver, and adipose tissues. KEGG (2021) pathway analysis ranked retinol metabolism highest, with additional enrichment in cytochrome P450-mediated metabolism of xenobiotics, fatty acids, and drugs. Reactome (2024) pathways included ethanol oxidation and bile acid recycling (see Figure 3).

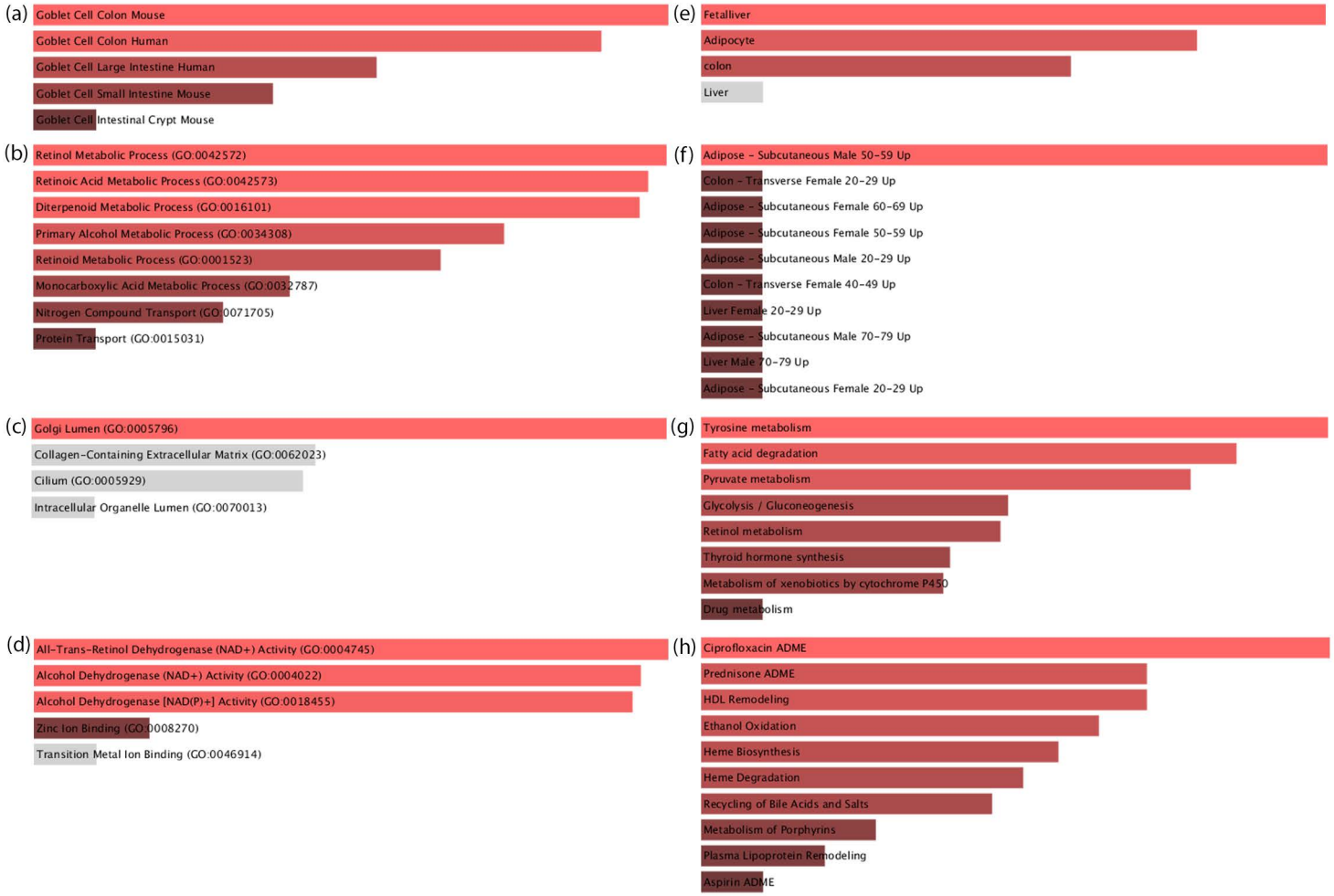

Figure 3 Functional enrichment and tissue-specific expression analysis of target genes. (a) Cell type marker enrichment (CellMarker_2024). (b-d) Gene Ontology (GO) enrichment for (b) biological processes, (c) cellular components, and (d) molecular functions (GO_2025). (e) Tissue-specific expression profiles from GTEx (v8, 2023). (f) Human Gene Atlas expression patterns across tissues. (g) KEGG pathway enrichment (2021 Human database). (h) Pathway enrichment analysis (Reactome_2024). Bar graphs depict the top enriched terms ranked by combined score ($-\log_{10}$(p-value) or Z-score). Data were analyzed using Enrichr (https://maayanlab.cloud/Enrichr/).

3.4 GeneMANIA Network Analysis

ALDH1A1, an essential enzyme in the retinoic acid synthesis process, was the subject of a functionally coherent module found in the GeneMANIA network (Figure 4). This network includes genes involved in lipid and alcohol metabolism and transport, as well as the three core differentially expressed genes (DEGs) seen in the Venn diagram (ALB, ZG16, and ADH1B). Alcohol dehydrogenases (ADH1A, ADH1B, and ADH1C) clustered together, emphasizing their cooperative roles in ethanol and retinol metabolism. Secretory proteins (ZG16, ALB, RBP4, AFP) were shown to form a distinct subnetwork, suggesting a possible function in mucosal defense and molecular transport. The fact that lipid transporters (FABP6, ABCC3) were connected to ALDH1A1 via solute carriers (SLC27A5, SLC01B1/B3) shows that retinoid processing and xenobiotic detoxification work together. This network highlights a functionally coherent module linking secretory activity, membrane transport, and retinoid metabolism.

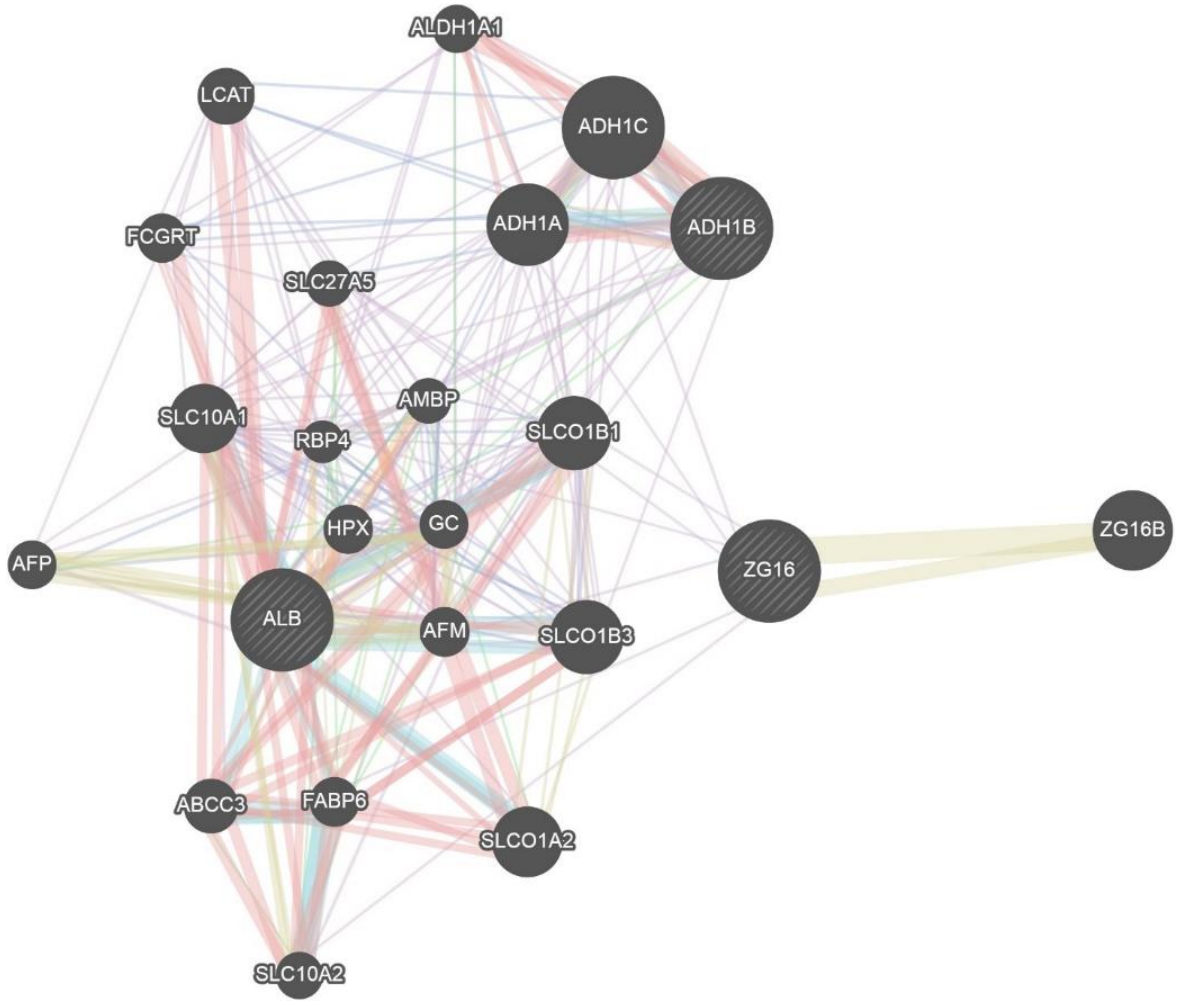

Figure 4 Protein-protein interaction network generated by GeneMANIA. Nodes represent genes/proteins colored by functional class (metabolic enzymes, transporters, etc.), while edges indicate interactions (co-expression, physical interactions, genetic interactions) with line thickness corresponding to confidence score.

3.5 Venn Diagram of Differentially Expressed Genes (DEGs)

The Venn diagram identified three genes (ADH1B, ZG16, and ALB) as commonly differentially expressed across the comparisons: liver metastases vs. normal liver (LM/NL), liver metastases vs. primary tumors (LM/PT), and liver transplantation vs. normal liver (LT/NL). These three genes occupied the central overlap, with minimal additional shared genes between other comparison pairs (Figure 5 and Table S1). Table S1 lists all genes identified in the Venn diagram intersections, categorized by their occurrence frequency across the four comparisons. Among these, ADH1B, ALB, and ZG16 were the only genes consistently dysregulated across all four comparisons (each appearing 4 times), confirming them as the core conserved molecular signature.

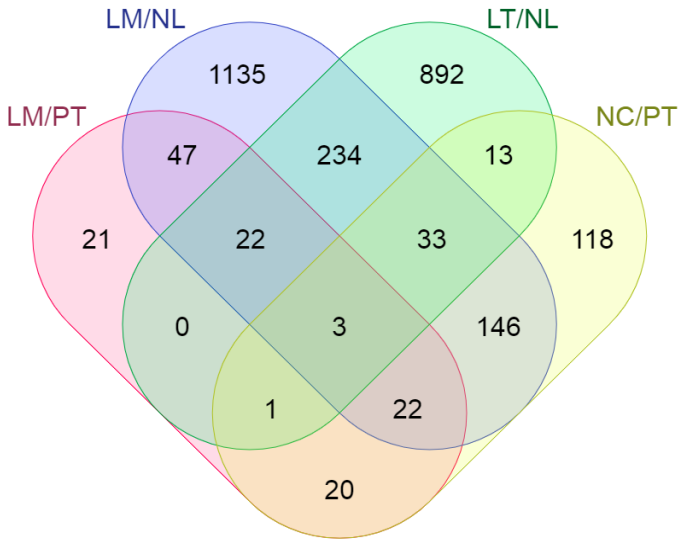

Figure 5 Venn diagram of the four groups to identify the shared genes among the target groups. The central overlap (n = 3 genes) represents ADH1B, ALB, and ZG16, which are dysregulated across all four comparisons. See Table S1 for complete gene lists for all intersections.

GeneMANIA network analysis placed these genes within a larger module containing ALDH1A1 and other genes involved in lipid/alcohol metabolism and transport (Figure 4).

3.6 Immune Infiltration Analysis

We investigated the relationship between gene expression and immune cell infiltration in the tumor microenvironment by looking at the expression levels of ADH1B, ZG16, and ALB using the TIMER 3.0 platform (Figure 6). Six other immune cell types-B cells, $CD8^+$ T cells, $CD4^+$ T cells, neutrophils, dendritic cells, and macrophages-were examined for association in addition to tumor purity. We included both partial correlations and the Spearman correlation coefficient to assess tumor purity.

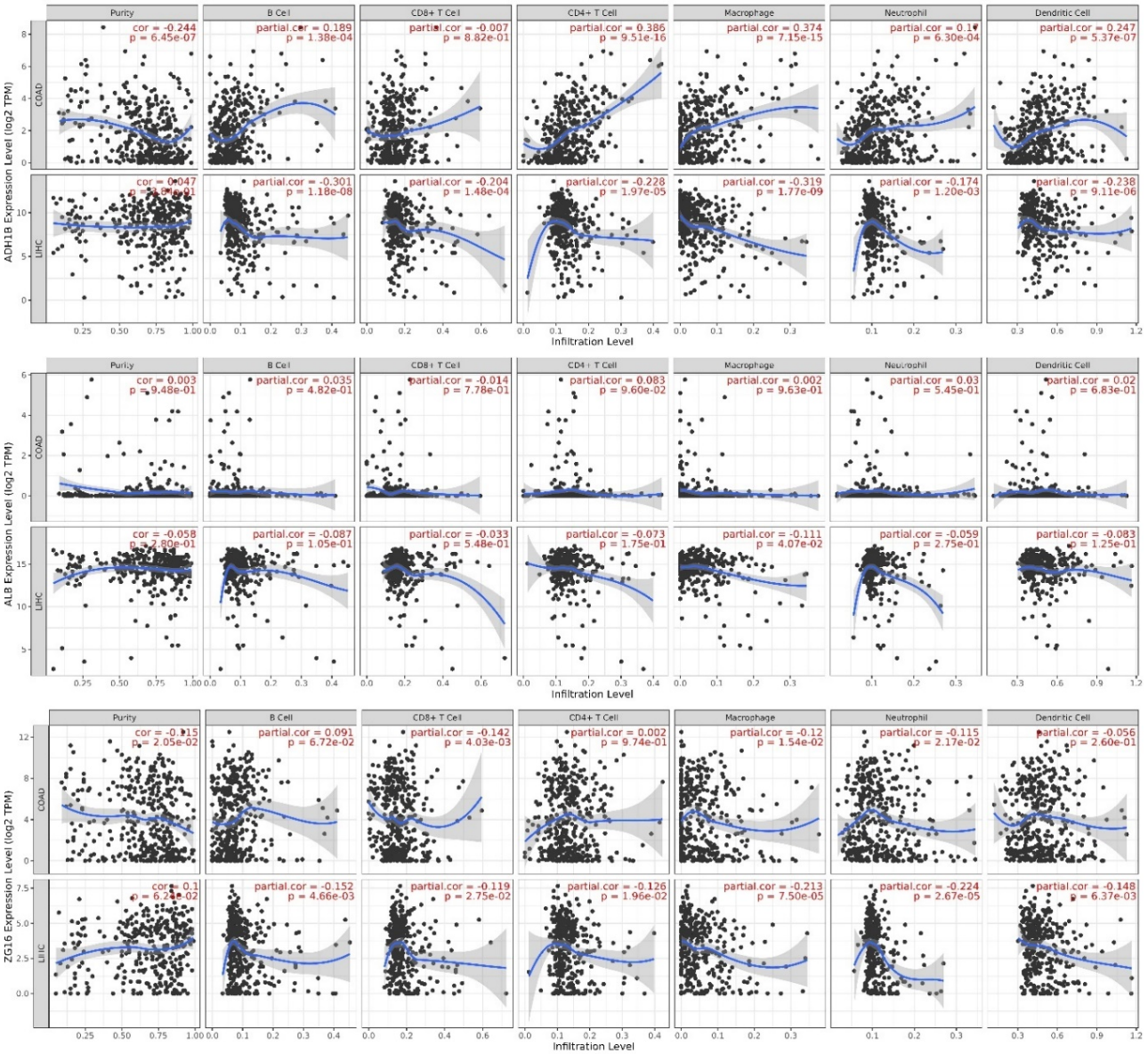

Figure 6 Scatter plots showing correlations between expression levels of ADH1B, ALB, and ZG16 (log_2 TPM) and immune cell infiltration levels in various cell types. Points represent samples, with blue trend lines and shaded confidence intervals. Red text shows correlation coefficients and p-values, indicating the strength and significance of these relationships in the tumor microenvironment.

Using TIMER 3.0, we assessed correlations between expression of ADH1B, ALB, and ZG16 (log_2 TPM) and immune cell infiltration.

ADH1B expression showed positive partial correlations with B cells (r = 0.189, p = 1.38e-4), $CD4^+$ T cells (r = 0.386, p = 7.15e-15), macrophages (r = 0.374, p = 6.3e-4), neutrophils (r = 0.171, p = 5.37e-7), and dendritic cells (r = 0.247, p = 5.37e-7). It was negatively correlated with tumor purity (r = -0.244, p = 6.45e-7).

ALB expression showed mostly weak or non-significant correlations, with a modest negative association with macrophages (r = -0.111, p = 4.07e-7).

ZG16 expression showed negative partial correlations with B cells (r = -0.152, p = 4.66e-3), $CD8^+$ T cells (r = -0.142, p = 4.03e-3), macrophages (r = -0.213, p = 7.5e-5), neutrophils (r = -0.224, p = 2.67e-5), and dendritic cells (r = -0.148, p = 6.37e-3) (Figure 6).

3.7 BATMAN-TCM Analysis of Herb and Ingredient Associations

3.7.1 Herb Enrichment Results

The herb enrichment investigation revealed that some botanicals linked to the gene set had significant enrichment ratios (Table 1). With 362.21, Rhizoma zingiberis praeparata (PAO JIANG) and Rhizoma zingiberis recens preparata (HEI JIANG) had the highest enrichment ratio. Tamarisk gallica (FA GUO CHENG LIU) and Clerodendron serratum (SAN TAI HONG HUA) came next with 258.72 and 258.72, respectively. These herbs show focused bioactivity, often associated with two target genes and one to three TCM components. Metabolic herbs including Daucus carota (HU LUO BO) and Schisandra chinensis (WU WEI ZI) were also found; the latter was linked to fourteen components, indicating a more intricate phytochemical profile.

Table 1 Enriched herbal medicines predicted by BATMAN-TCM analysis.

Herb (Latin)	Herb (Pinyin)	#TCM ingredients	#Genes	Enrichment ratio
Rhizoma zingiberis praeparata	PAO JIANG	3	2	362.21
Rhizoma zingiberis recens preparata	HEI JIANG	3	2	362.21
Clerodendron serratum	SAN TAI HONG HUA	1	2	258.72
Phasianus colchicus	ZHI	1	2	258.72
Tamarix gallica	FA GUO CHENG LIU	1	2	258.72
Veronica spuria	YI ZHI XIANG	1	2	222.41
Plagiochasma intermedium	WU WEN ZI BEI TAI	2	2	195.04
Ulex sp.	None	1	2	154.6
Dioscorea sp.	None	1	2	154.6
Russula lepida	DA HONG GU	1	2	154.6
Blumea lacera	HONG TOU CAO	1	2	152.74
Rosa sp.	None	1	2	150.92
Daucus carota var. sativa	HU LUO BO	3	2	147.41
Ipomoea batatas [syn. convolvulus batatas]	GAN SHU	3	2	145.72
Narcissus tazetta	DUO HUA SHUI XIAN	1	2	142.44
Carica papaya	FAN MU GUA	5	2	129.36
Veronicastrum sibiricum	ZHAN LONG JIAN	1	2	124.29
Picrorhiza scrophulariiflora	XI ZANG HU HUANG LIAN	1	2	123.08
Elaeis guineensis	YOU ZONG	1	2	113.19
Brandisia hancei	LAI JIANG TENG	4	2	89.91
Sonchus arvensis	NIU SHE TOU	1	2	88.65
None	XIAN TAO CAO	2	2	82.32

Aloe vera var. chinensis	BAN WEN LU HUI	3	2	77.78
Flos dolichoris	BIAN DOU HUA	1	2	77.78
Polyporus umbellatus	ZHU LING	1	2	72.86
Capsicum annuum	HONG HAI JIAO	3	2	71.62
Flos chrysanthemi	HANG JU	1	2	71.22
Eucalyptus globulus	AN YE	3	2	71.22
Anethum graveolens	SHI LUO ZI	7	2	66.37
Gardenia jasminoides var. grandiflora	SHUI ZHI	3	2	64.03
Rehmannia glutinosa [syn. rehmannia glutinosa f. huechingensis]	XIAN DI HUANG	1	2	60.08
Schisandra chinensis	WU WEI ZI	14	2	59.24
Piper longum	BI BA	10	2	57.36
None	SONG ZI REN	1	2	55.85
Cistanche tubulosa	GUAN HUA ROU CONG RONG	4	2	55.12
Radix chuanxiong; rhizoma chuanxiong	XI CHUAN XIONG	7	2	53.95
Acanthopanax giraldii [syn. acanthopanax giraldii var. inermis, eleutherococcus giraldii]	HONG MAO WU JIA PI	8	2	50.91
Polygala tenuifolia	YUAN ZHI	2	2	50.31
Aralia decaisneaa	HUANG MAO CONG MU	2	2	45.93
Armillariella mellea	ZHEN MO	4	2	45.12
Aristolochia manshuriensis	GUAN MU TONG	2	2	42.97
Lablab niger	BIAN DOU	1	2	42.4
Oplopanax elatus	DONG BEI CI REN SHEN	13	2	41.29
Rhodiola crenulata [syn. rhodiola euryphylla]	DA HUA HONG JING TIAN	2	2	41.16
None	JU LUO	4	2	40.89
Daucus carota	NAN HE SHI	15	2	40.5
Zea mays	YU SHU SHU	1	2	40.5
Sargassum	HAI ZAO	1	2	40.37
None	ZI HUA QIAN HU	3	2	39.99
Ophiopogon japonicus	MAI DONG	3	2	39.99

3.7.2 Ingredient Enrichment and Core Gene Targeting

Investigation at the constituent level revealed high relationships with the critical genes ADH1B and ALB. Beta-carotene is known to be an ALB target, and both D-mannitol (enrichment ratio: 189.21) and beta-carotene (114.21) had strong binding to ALB and ADH1B. As a well-known ALB binder, the component “7440-69-9” stood out with an outstanding enrichment ratio of 6,338.67. Aristololactam GII and phenolic compounds such as 4-Methoxyphenol and Schisanhenol were

among the alkaloids and phenolic compounds found in ALB consistently, suggesting albumin's crucial role as a transporter for several phytochemicals.

3.7.3 Gene-Ingredient Network Complexity

Gene-ingredient mapping verified the complete targeting of ADH1B and ALB. ADH1B was predicted to interact with several compounds, including candidates with high BATMAN scores (≥0.84). Similarly, ALB interacted with various components, with two known targets (PubChem IDs: 5280489 and 5359367), and some of which were designated as targets (e.g., beta-carotene and D-mannitol), and others had high affinity values. This broad network reveals ADH1B and ALB as essential nodes for the effect of TCM compounds, which is consistent with their previously identified roles in retinoid metabolism and detoxification in enrichment studies (Table 2).

Table 2 Enriched herbal ingredients identified using BATMAN-TCM analysis.

PubChem_ID	TCM ingredients	Enrichment_ratio	Associated_Genes
6251	D-mannitol	189.21	ALB(0.94)|ADH1B(0.84)
5280489	beta-carotene	114.21	ALB(known target)| ADH1B(0.84)
453	Hexitol	108.35	ALB(0.94)|ADH1B(0.84)
5359367	7440-69-9	6338.67	ALB(known target)
5319480	4-Methoxyphenanthrene-2,3,7-triol	6338.67	ALB(0.89)
5319479	4-Methoxyphenanthrene-2,3,6,7-tetrol	6338.67	ALB(0.89)
9982511	Blestriarene C	3169.33	ALB(0.84)
96038	2,6-dimethoxybenzene-1,4-diol	3169.33	ALB(0.84)
91542987	Isoarundinin II	3169.33	ALB(0.84)
9015	4-Methoxyphenol	3169.33	ALB(0.89)
9007	3-METHOXYPHENOL	3169.33	ALB(0.84)
87579595	SCHEMBL3814594	3169.33	ALB(0.84)
87579315	SCHEMBL3812956	3169.33	ALB(0.84)
85243417	85243417	3169.33	ALB(0.84)
85243417	Litcubine	3169.33	ALB(0.84)
8456	2-tert-Butyl-4-methoxyphenol	3169.33	ALB(0.84)
73057	Schisanhenol	3169.33	ALB(0.84)
71573815	Aristololactam GII	3169.33	ALB(0.84)
7144	2-METHOXY-4-METHYLPHENOL	3169.33	ALB(0.84)
71375357	3-[2-(4-Methoxyphenyl)ethyl]phenol	3169.33	ALB(0.84)
7041	2,6-DIMETHOXYPHENOL	3169.33	ALB(0.89)
69988	2-Methoxyhydroquinone	3169.33	ALB(0.89)
69505	3,4,5-Trimethoxyphenol	3169.33	ALB(0.84)
67233527	SCHEMBL1974074	3169.33	ALB(0.84)
6713072	NCIMech_000339	3169.33	ALB(0.84)
642896	STILBOSTEMIN E	3169.33	ALB(0.84)
641760	Stemanthrene A	3169.33	ALB(0.84)
636881	Coeloginanthridin	3169.33	ALB(0.84)

60205844	7-methoxy-3-methyl-9,10-dihydrophenanthrene-2,5-diol	3169.33	ALB(0.84)
580771	3-Ethoxy-4-methoxyphenol	3169.33	ALB(0.84)
53220714	856451-92-8	3169.33	ALB(0.84)
5321921	2,4-dimethoxy-6-tricosylphenol	3169.33	ALB(0.84)
5320703	Isopregomisin	3169.33	ALB(0.84)
5320553	Picrasidine J	3169.33	ALB(0.84)
5317966	13,15-dimethoxy-10-azatetracyclo [7.6.1.02,7.012,16]hexadeca-1(16), 2,4,6,8,12,14-heptaen-11-one	3169.33	ALB(0.84)
5317823	Griffithinam	3169.33	ALB(0.84)
5317805	Gomisin K2, (+)-	3169.33	ALB(0.84)
5316861	2-(1,7-dihydroxy-6,8-dimethoxy-3-methyl-5-propan-2-ylnaphthalen-2-yl)-6,8-dimethoxy-3-methyl-5-propan-2-ylnaphthalene-1,7-diol	3169.33	ALB(0.84)
5315860	Chrysotoxine	3169.33	ALB(0.84)
5315859	7-hydroxy-2,3,4,8-tetramethoxyphenanthrene	3169.33	ALB(0.84)
5315503	Broussonin B	3169.33	ALB(0.84)
5315502	Broussonin A	3169.33	ALB(0.84)
489939	Kalasinamide	3169.33	ALB(0.84)
46879743	495416-58-5	3169.33	ALB(0.84)
46871897	3,4,8-trimethoxyphenanthrene-2,5-diol	3169.33	ALB(0.84)
44567164	broussonin F	3169.33	ALB(0.84)
44422603	Oldhamactam	3169.33	ALB(0.84)
44392564	CHEMBL181587	3169.33	ALB(0.84)
44392553	CHEMBL181441	3169.33	ALB(0.84)
442711	3’-O-Methylbatatasin III	3169.33	ALB(0.84)

3.7.4 Synthesis

The BATMAN-TCM findings showed two key themes: first, high-specificity herbs (such as PAO JIANG and SAN TAI HONG HUA) exhibit concentrated bioactivity because of their high enrichment ratios and low component counts. In addition to chemicals like beta-carotene and D-mannitol that target a variety of processes, key genes like ADH1B and ALB combine metabolic, detoxifying, and carrier functions. These findings indicate which ingredients and plants need to be examined in a hepatic and gastrointestinal context to verify their effectiveness.

3.8 Compound-Gene Interaction Analysis via BATMAN-TCM 2.0

To investigate the connections between regulatory compounds and ALB and ADH1B, we searched BATMAN-TCM 2.0 for known or anticipated relationships between each gene and small molecules, especially natural products that are often used in traditional Chinese medicine (Figure 7). ALB showed a wide range of chemical interactions, including robust relationships (red edges)

with bioactive substances such as oxybuprocaine, hydrocortisone, beta-carotene, resveratrol, curcumin, and piperine. ALB's potential as a broadly responsive gene to bioactive metabolic modulators is highlighted by its reported roles in modulating oxidative stress, immunological signaling, and hepatic function.

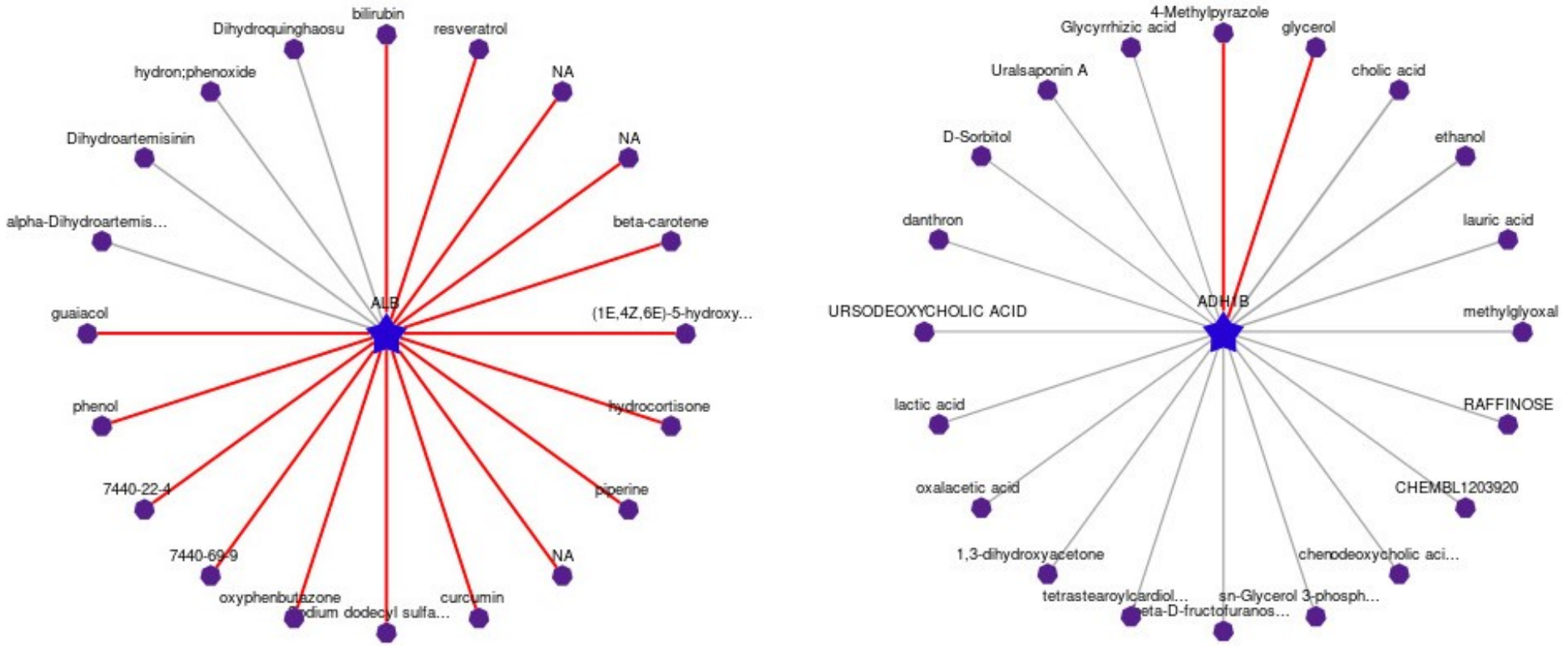

Figure 7 Network diagrams showing the molecular interactions of ALB (left) and ADH1B (right) with various chemical compounds. Red lines represent strong associations, while grey lines indicate weaker or unconfirmed links.

In contrast, ADH1B showed fewer compound interactions, but they were more specific. Strong predicted interactions were identified with 4-methylpyrazole and glycerol, two substances related to the inhibition of alcohol dehydrogenase and alcohol metabolism, respectively. Weak interactions with ursodeoxycholic acid, glycyrrhizic acid, and cholic acid may indicate a functional niche related to bile acid or detoxification pathways. The fact that ZG16 did not produce any compound interaction data in BATMAN-TCM 2.0 shows that bioactives derived from traditional medicine have been poorly characterized.

4. Discussion

In this study, we identified consistent dysregulation of three genes-ADH1B, ALB, and ZG16-across primary colorectal tumors, liver metastases, and post-liver transplantation hepatic tissue. These genes emerged as the only common differentially expressed genes (adjusted $p < 0.05$, $|logFC| > 1.5$) shared among the key comparisons (LM vs. NL, LM vs. PT, and LT vs. NL), highlighting a conserved molecular signature linking colorectal cancer progression, metastatic colonization of the liver, and the post-transplant hepatic microenvironment.

These three genes may define a candidate immunometabolic network that integrates retinoid and alcohol metabolism, mucosal barrier function, systemic transport, and modulation of the immune microenvironment. ADH1B, a key enzyme in retinol and ethanol oxidation, showed positive correlations with infiltration of multiple immune cell types (B cells, $CD4^+$ T cells, macrophages, neutrophils, and dendritic cells) and a negative correlation with tumor purity. The positive correlations suggest that ADH1B expression is associated with immune infiltration, supporting a potential role in the immune microenvironment. In contrast, ZG16 exhibited consistent negative correlations with immune cell infiltration, consistent with its role in maintaining goblet cell function and intestinal mucosal integrity; its downregulation may facilitate immune exclusion and promote a tumor-permissive or graft-tolerant environment. ALB, a major carrier of fatty acids, retinoids, and xenobiotics, may represent an important integrator of metabolic status and systemic inflammation, as evidenced by its known clinical utility in CRP/ALB ratios for prognosis in both cancer and transplantation settings.

This immunometabolic convergence has important implications for colorectal cancer recurrence after liver transplantation. Immunosuppressive regimens impair anti-tumor surveillance while simultaneously altering hepatic metabolic capacity. The co-dysregulation of ADH1B, ALB, and ZG16 may represent a molecular bridge whereby metabolic reprogramming (Warburg-like shifts, retinoid imbalance) and barrier dysfunction converge to weaken immune control, thereby facilitating metastatic outgrowth in the immunosuppressed host. This model integrates previously fragmented observations in CRC immunobiology and transplant oncology and provides a conceptual framework for future mechanistic investigation.

Beyond biomarker potential, our findings highlight ADH1B and ALB as particularly promising therapeutic nodes. BATMAN-TCM predicted that both genes interact with several bioactive dietary compounds, opening avenues for adjunctive interventions. Network pharmacology analysis (BATMAN-TCM 2.0) identified strong associations between these genes and natural compounds such as beta-carotene, resveratrol, curcumin, and D-mannitol.

These compounds collectively target multiple layers of the identified axis: beta-carotene supports retinoid signaling and antioxidant defense; resveratrol and curcumin exert potent anti-

inflammatory and immunomodulatory effects via NF-κB, STAT3, and p53 pathways; and D-mannitol provides osmotic and ROS-scavenging support that may mitigate ischemia-reperfusion injury in the graft. These compounds represent candidates for future validation because of their reported immunomodulatory and metabolic effects. Whether they act synergistically to restore immunometabolic balance, enhance anti-tumor immunity, or support graft tolerance and function remains to be tested experimentally. This integrated strategy warrants further investigation because several of these compounds have established safety profiles and documented biological activities and could be used as low-risk adjuncts to standard immunosuppression and surveillance protocols.

Future studies should validate these compound-gene interactions in relevant preclinical models (e.g., CRC organoids co-cultured with immune cells under immunosuppressive conditions) and explore whether modulating this axis can reduce recurrence rates or improve graft outcomes in clinical cohorts. Longitudinal monitoring of ADH1B and ALB expression (in tissue or liquid biopsy) may also serve as early indicators of recurrence risk.

In some carefully selected patients, unresectable colorectal liver metastases (CRLM) are an emerging option for liver transplantation. However, within the post-transplant setting, recurrence of CRC is still a big challenge as a result of immunosuppressive therapy. The fact that we identified a conserved immunometabolic signature (ADH1B, ALB, ZG16) across primary CRC, CRLM lesions, and post-LT liver tissue provides a plausible molecular explanation for the increased risk of recurrence in this setting; these genes could serve as markers for better post-transplant surveillance. These findings may inform patient selection and surveillance in emerging LT programs for unresectable CRLM, such as those following the SECA criteria or RAPID protocol, by providing molecular readouts of immunometabolic status that could complement current clinical risk stratification.

Alcohol dehydrogenase 1B (ADH1B) has been implicated in cancer biology, including potential roles in immunological modulation in hepatocellular carcinoma [47]. The ADH1B*2 variation, which alters retinol, alcohol, and lipid peroxidation product metabolism, is associated with an increased risk of colorectal cancer (CRC) [48]. In hepatocellular carcinoma, ADH1B has been associated with immune modulation [47]. Similar mechanisms may operate in colorectal cancer, though this requires further investigation. The enzyme ADH1B has a role in immunological function and cancer risk; in certain individuals, dietary interactions, especially with folate, further complicate metabolic and immune pathways [48].

ZG16 improves gut mucosal immunity in two ways: it prevents microbial invasion and preserves epithelial integrity. ZG16 deletion promotes inflammation and stem-like CRC cell proliferation, both of which accelerate tumor development [49, 50]. Because of its structural resemblance to Jacalin, it is thought to have a role in immunological signaling; its absence weakens mucosal defenses and may worsen inflammation and dysbiosis [50]. The gut-liver axis plays a critical role in immune regulation after liver transplantation, and disruption of mucosal integrity may contribute to increased risk of rejection and infection [51].

Albumin (ALB) is an important biomarker for assessing systemic inflammation and immunological competency [52]. The CRP/ALB ratio has been shown to reliably predict outcomes in colorectal cancer [53, 54], and similar inflammation-based markers have prognostic value in liver transplantation [55]. Insufficient albumin synthesis has been linked to increased overall morbidity

and longer hospital stays in liver transplant recipients, highlighting its role as a marker of poor post-transplant outcomes [56].

Colorectal cancer (CRC) and liver transplant immunology share immune escape mechanisms including ALB, ZG16, and ADH1B. Reduced ALB indicates an inflammatory, immunosuppressive environment, loss of ZG16 impacts mucosal protection, and dysregulated ADH1B alters immune metabolism. Together, these changes may contribute to tumor progression, complicate immune surveillance, and hinder transplant recovery [49, 54, 57].

The Warburg effect, a metabolic reprogramming process, causes metabolism to shift toward aerobic glycolysis, which encourages the growth of tumors in hepatocellular carcinoma (HCC) and colorectal cancer (CRC). This lowers anti-tumor immunity and creates an immunosuppressive tumor microenvironment [58, 59]. Liver transplantation's metabolic requirements also impact systemic immunity, making immunological tolerance and recovery more challenging [60, 61]. Focusing on these metabolic pathways may improve transplant outcomes and immunotherapy responses.

Beta-carotene has context-dependent biological effects, with an intricate role in liver transplantation and a correlation with the prevention of colorectal cancer (CRC). Epidemiological studies have shown a decreased incidence of colon cancer with higher nutritional intake, especially in nonsmokers [62, 63]. However, since beta-carotene acts as a pro-oxidant and exacerbates oxidative stress, it may raise the risk of cancer in smokers [64-66]. After transplantation, beta-carotene may enhance immunological function and reduce oxidative damage to promote graft survival and immune homeostasis [67]. Beta-carotene may improve graft survival and immune balance by increasing immunological function and reducing oxidative damage following transplantation [68, 69]. These two outcomes underscore the significance of context-appropriate beta-carotene usage in post-transplant care and cancer prevention.

Resveratrol, a polyphenol found in berries and grapes, has demonstrated promising chemopreventive effects in colorectal cancer (CRC) and liver transplantation. It regulates key tumor-related pathways, inhibits cell proliferation, and increases apoptosis in colorectal cancer [70-72]. By activating tumor suppressors like p53 and blocking signals linked to invasion and inflammation, it also increases its chemopreventive effectiveness [73]. Furthermore, epidemiological research shows that consuming more resveratrol in the diet is connected with a decreased risk of colon cancer [74]. Resveratrol has demonstrated hepatoprotective effects in murine liver ischemia-reperfusion models by attenuating ischemia-reperfusion injury and improving graft function [75]. Its antioxidant and anti-inflammatory properties also reduce complications such as rejection and infection [76]. Resveratrol is a potential therapeutic agent for colorectal cancer prevention and post-transplant recovery owing to its dual benefits.

The bioactive component curcumin, which is found in turmeric, has shown therapeutic potential in the treatment of liver transplantation and colorectal cancer (CRC). Through apoptosis induction, proliferation inhibition, and modulation of inflammatory signaling, including NF-κB and STAT3, curcumin inhibits the growth and spread of colorectal cancer tumors [77-79]. Additionally, since it boosts the efficacy of chemotherapeutics like oxaliplatin and 5-fluorouracil, it is helpful in combination therapy [80, 81]. By reducing oxidative stress and inflammatory indicators, curcumin provides hepatoprotective advantages to liver transplant patients, especially when ischemia-reperfusion injury (IRI) is present [82-85]. Its therapeutic usefulness is limited by its low absorption, but it improves graft maintenance and outcomes. Improved delivery techniques or adjuvants like

piperine may assist in overcoming this restriction [81, 86, 87]. These studies show that curcumin might be a multi-target medication for colorectal cancer and liver transplantation.

D-mannitol, a sugar alcohol widely used as an osmotic agent, has demonstrated utility in liver transplantation. Mannitol's antioxidant properties help in tissue perfusion and healing after surgery or transplantation [88-90]. Mannitol is an osmotic diuretic that may aid in postoperative recovery and has been investigated for its effects on intraoperative perfusion [90]. In liver transplantation, mannitol can reduce the incidence of post-reperfusion syndrome and aid in kidney perfusion while scavenging reactive oxygen species [89]. Proper timing of delivery, such as shortly after cross-clamping, may increase graft function and overall transplant outcomes [88, 89]. Its cytoprotective activities may contribute to improved graft preservation and reduced complications [90].

Bioactive substances (beta-carotene, resveratrol, curcumin, and D-mannitol) and genes (ALB, ZG16, and ADH1B) affect the genesis of colorectal cancer and the effectiveness of liver transplants. These findings highlight the need for coordinated therapeutic approaches that address both metabolic and immune regulation, as highlighted by the interdependent roles of cancer and transplantation in enhancing outcomes.

Our study's findings complement and enhance the corpus of information already available on the immunobiology of liver transplants and colorectal cancer. Our multi-omics methodology indicates that retinoid metabolism and regulation of the mucosal barrier also play a convergent role, even while immunological checkpoint signaling, metabolic reprogramming, and immunosuppressive therapy are known to promote the development of colorectal cancer. A shared pathway of metabolic-immune dysfunction facilitated by secretory and detoxifying systems is highlighted by the interrelated dysregulation of ADH1B, ALB, and ZG16 in tumor and transplant contexts. Furthermore, the anticipated interactions between core genes and bioactive substances like beta-carotene and D-mannitol bring additional regulatory mechanisms. This approach uses both modern and conventional pharmacology to identify potential intervention targets.

This research's fundamental novelty is its tri-contextual integration, which simultaneously examines gene expression in primary colorectal tumors, hepatic metastases, and liver transplant tissues. While research has examined each of these biological environments independently, little is understood about their interactions. Through the identification of a simple but potent gene signature-ADH1B, ALB, and ZG16-shared by all three disorders, our study identifies a previously unrecognized molecular convergence point linking immunological escape, tumor formation, and transplant-mediated immune regulation. Our findings place tumors, hosts, and grafts in a broader context beyond cancer and transplant immunology and provide important new insights into the metabolic and immunological regulatory networks that they all share.

Several limitations should be taken into account, even if this work offers insightful information on the common immuno-metabolic characteristics that connect colorectal cancer, liver metastases, and liver transplantation. First, the research may be limited in its statistical power and generalizability due to its reliance on publicly accessible transcriptome datasets for liver transplant tissues that have very small sample sizes. Second, even though multi-omics integration made it possible to conduct thorough pathway and network studies, our capacity to resolve immunological heterogeneity and cell-type-specific gene regulation in the tumor microenvironment and graft tissues is limited by the absence of single-cell resolution. Third, while useful, the BATMAN-TCM predictions for compound-gene interactions are computationally derived and need experimental confirmation to verify binding selectivity, bioactivity, and in vivo relevance. Furthermore, one of the

identified key genes, ZG16, lacks thorough functional annotation in immunological and hepatic settings, which means that its functional role remains incompletely understood. Last but not least, this study ignores patient-level clinical heterogeneity that may affect gene expression and immunological dynamics in actual transplant patients, such as age, sex, comorbidities, or immunosuppressive regimens. To confirm gene function and compound effects in CRC and transplant models, future research should use experimental assays, larger, clinically annotated cohorts, and longitudinal multi-omics.

To expand on this study's conclusions, further research is needed in several crucial areas. The application of single-cell and spatial transcriptomic technologies might be the next step in determining the cellular and geographic specificity of ADH1B, ALB, and ZG16 expression in primary colorectal malignancies, liver metastases, and transplanted liver tissues. These strategies could help us better understand the microenvironmental heterogeneity and immune-epithelial interactions that drive tumor development and immune modulation after transplant. Second, we need to validate the compound-gene interactions suggested by BATMAN-TCM. This is notably true for phytochemicals such as beta-carotene and D-mannitol. Still, it could also be done using in vitro models such as hepatocyte cultures, colorectal cancer cell lines, or co-culture systems including immune cells. The functional implications of chemical binding and the regulatory influence of these bioactives on important immunometabolic pathways can only be evaluated using these tests. Finally, clinical studies should be conducted to determine if ALB and ADH1B may be utilized as biomarkers to predict the recurrence of colorectal cancer following liver transplantation. Their expression levels in peripheral blood or biopsy samples might aid in risk assessment and monitoring after transplant. These future projects are coming together with the objective of assisting individuals with colorectal cancer and liver transplant patients in receiving individualized therapeutic treatments by reducing the gap between molecular discovery and translational application.

All of these findings hint at a core immunometabolic axis involved in colorectal cancer development and recurrence after transplantation. ADH1B and ALB stand out as two genes with many similarities at the intersection of tumor metabolism, immune control, and liver function, and they might be promising candidates for therapeutic modulation and more mechanistic research.

5. Conclusions

This study identifies a candidate shared immunometabolic axis involving the consistent dysregulation of ADH1B, ALB, and ZG16 across primary colorectal tumors, liver metastases, and post-liver transplantation hepatic tissue. These genes integrate critical processes including retinoic acid and alcohol metabolism, mucosal barrier maintenance, detoxification, and modulation of immune cell infiltration.

ADH1B and ALB emerge as promising candidate biomarkers for future clinical translation. If validated prospectively, ALB, as a routinely measured serum protein, could be integrated into post-transplant surveillance protocols. For example, serial monitoring of serum ALB levels combined with the CRP/ALB ratio may help identify patients at elevated risk of CRC recurrence early after liver transplantation. A declining ALB trend or persistently low levels could trigger intensified imaging or liquid biopsy screening for metastatic disease. Similarly, hepatic or circulating ADH1B expression (assessed via qPCR or immunohistochemistry on biopsies) may eventually serve as a complementary

marker of immunometabolic imbalance and recurrence risk, especially in patients with MSS/pMMR tumors that respond poorly to current immunotherapies.

To advance clinical application, future validation studies should include prospective longitudinal cohorts of liver transplant recipients with a history of CRC, multicenter studies incorporating liquid biopsy approaches, and functional validation using patient-derived organoids and appropriate animal models.

We acknowledge important limitations of the current work. The analysis relied on publicly available transcriptomic datasets with a notably small sample size for liver transplantation samples (n = 5 per group in GSE14951), which limits statistical power and generalizability. Additionally, the bulk RNA-seq approach lacks single-cell resolution, preventing detailed characterization of cell-type-specific expression and microenvironmental interactions. Finally, the compound-gene interactions predicted by BATMAN-TCM 2.0 are based on computational network pharmacology and require experimental confirmation of binding affinity, bioactivity, and therapeutic efficacy in relevant biological models.

Despite these limitations, our findings provide a unified framework for tumor-host-graft interactions and highlight natural compounds (curcumin, beta-carotene, resveratrol, and D-mannitol) as potential low-risk adjunctive modulators of this immunometabolic axis. Future research combining single-cell and spatial transcriptomics, preclinical organoid and animal models, and well-designed prospective clinical cohorts will be essential to translate these insights into precision strategies that improve outcomes in colorectal cancer patients undergoing liver transplantation.

Acknowledgments

The authors would like to thank the Research Office of Tabriz University of Medical Sciences for approval and support of the study under PAZHOUHAN tracking number 79284.

Author Contributions

EA carried out the gathering and analyzing of studies. BS participated in the design of the study and drafted the manuscript. EA and BS conceived of the study and participated in its design and coordination as well as the analyses of data. All authors read and approved the final manuscript.

Competing Interests

The authors have declared that no competing interests exist.

Additional Materials

The following additional materials are uploaded at the page of this paper.

1. Table S1: Complete list of genes identified in Venn diagram intersections across all four comparisons.

References

1. Shi Y, Zou Z, Kerr D. Why don't immune checkpoint inhibitors work in colorectal cancer. J Gastrointest Cancer Stromal Tumor. 2017; 2: 114.
2. Topalian SL, Drake CG, Pardoll DM. Immune checkpoint blockade: A common denominator approach to cancer therapy. Cancer Cell. 2015; 27: 450-461.
3. Sahin IH, Akce M, Alese O, Shaib W, Lesinski GB, El-Rayes B, et al. Immune checkpoint inhibitors for the treatment of MSI-H/MMR-D colorectal cancer and a perspective on resistance mechanisms. Br J Cancer. 2019; 121: 809-818.
4. Pardoll DM. The blockade of immune checkpoints in cancer immunotherapy. Nat Rev Cancer. 2012; 12: 252-264.
5. Janssen E, Subtil B, de la Jara Ortiz F, Verheul HM, Tauriello DV. Combinatorial immunotherapies for metastatic colorectal cancer. Cancers. 2020; 12: 1875.
6. Llosa NJ, Luber B, Tam AJ, Smith KN, Siegel N, Awan AH, et al. Intratumoral adaptive immunosuppression and type 17 immunity in mismatch repair proficient colorectal tumors. Clin Cancer Res. 2019; 25: 5250-5259.
7. Tauriello DV, Palomo-Ponce S, Stork D, Berenguer-Llergo A, Badia-Ramentol J, Iglesias M, et al. TGFβ drives immune evasion in genetically reconstituted colon cancer metastasis. Nature. 2018; 554: 538-543.
8. Zhang H, Wang Y, Onuma A, He J, Wang H, Xia Y, et al. Neutrophils extracellular traps inhibition improves PD-1 blockade immunotherapy in colorectal cancer. Cancers. 2021; 13: 5333.
9. Grasso CS, Giannakis M, Wells DK, Hamada T, Mu XJ, Quist M, et al. Genetic mechanisms of immune evasion in colorectal cancer. Cancer Discov. 2018; 8: 730-749.
10. Bagchi S, Yuan R, Engleman EG. Immune checkpoint inhibitors for the treatment of cancer: Clinical impact and mechanisms of response and resistance. Annu Rev Pathol. 2021; 16: 223-249.
11. Rosenbaum MW, Bledsoe JR, Morales-Oyarvide V, Huynh TG, Mino-Kenudson M. PD-L1 expression in colorectal cancer is associated with microsatellite instability, BRAF mutation, medullary morphology and cytotoxic tumor-infiltrating lymphocytes. Mod Pathol. 2016; 29: 1104-1112.
12. Miyamoto Y, Ogawa K, Ohuchi M, Tokunaga R, Baba H. Emerging evidence of immunotherapy for colorectal cancer. Ann Gastroenterol Surg. 2023; 7: 216-224.
13. Le DT, Uram JN, Wang H, Bartlett BR, Kemberling H, Eyring AD, et al. PD-1 blockade in tumors with mismatch-repair deficiency. N Engl J Med. 2015; 372: 2509-2520.
14. Zeng T, Fang X, Lu J, Zhong Y, Lin X, Lin Z, et al. Efficacy and safety of immune checkpoint inhibitors in colorectal cancer: A systematic review and meta-analysis. Int J Colorectal Dis. 2022; 37: 251-258.
15. Ganesh K, Stadler ZK, Cercek A, Mendelsohn RB, Shia J, Segal NH, et al. Immunotherapy in colorectal cancer: Rationale, challenges and potential. Nat Rev Gastroenterol Hepatol. 2019; 16: 361-375.
16. Nicolaas JS, De Jonge V, Steyerberg EW, Kuipers EJ, Van Leerdam ME, Veldhuyzen-van Zanten SJO. Risk of colorectal carcinoma in post-liver transplant patients: A systematic review and meta-analysis. Am J Transplant. 2010; 10: 868-876.

17. Hagness M. Liver transplantation in treatment of colorectal liver metastases. Hepat Oncol. 2015; 2: 181-190.
18. Silva MA, Jambulingam PS, Mirza DF. Colorectal cancer after orthotopic liver transplantation. Crit Rev Oncol Hematol. 2005; 56: 147-153.
19. Gutierrez-Dalmau A, Campistol JM. Immunosuppressive therapy and malignancy in organ transplant recipients: A systematic review. Drugs. 2007; 67: 1167-1198.
20. Park HY, Chang BJ, Lim SW, Kim J, Kim JY, Chang DK, et al. Risk of colorectal neoplasia in patients with solid organ transplantation. Clin Transplant. 2012; 26: 50-56.
21. Zou Z, Tao T, Li H, Zhu X. mTOR signaling pathway and mTOR inhibitors in cancer: Progress and challenges. Cell Biosci. 2020; 10: 31.
22. Udaikumar J, Achuta KM, Lella VV, Nimmagadda R, Kuppili S, Tummala N, et al. Prevalence and risk factors of colorectal cancer in solid organ transplant recipients: A systematic review and meta analysis. Clin Transplant. 2026; 40: e70470.
23. Safaeian M, Robbins HA, Berndt SI, Lynch CF, Fraumeni Jr JF, Engels EA. Risk of colorectal cancer after solid organ transplantation in the United States. Am J Transplant. 2016; 16: 960-967.
24. Sung PS, Han JW, Seo C, Ahn J, Lee SK, Nam HC, et al. Real-life experience of mTOR inhibitors in liver transplant recipients in a region where living donation is predominant. Front Pharmacol. 2021; 12: 685176.
25. Shibuya N, Inoue KI, Tanaka G, Akimoto K, Kubota K. Augmented pentose phosphate pathway plays critical roles in colorectal carcinomas. Oncology. 2015; 88: 309-319.
26. Koseki Y, Kamimura K, Tanaka Y, Ohkoshi-Yamada M, Zhou Q, Matsumoto Y, et al. Rapid progression of colonic mucinous adenocarcinoma with immunosuppressive condition: A case report and review of literature. World J Clin Cases. 2021; 9: 9182-9191.
27. Liu Z, Ang MY, Kue CS. Multi omics integration in colorectal cancer: From molecular insights to precision oncology. Cancers. 2026; 18: 1504.
28. Johnson AC, Silva JAF, Kim SC, Larsen CP. Progress in kidney transplantation: The role for systems immunology. Front Med. 2022; 9: 1070385.
29. Shen Y, Xiong W, Gu Q, Zhang Q, Yue J, Liu C, et al. Multi-omics integrative analysis uncovers molecular subtypes and mRNAs as therapeutic targets for liver cancer. Front Med. 2021; 8: 654635.
30. Gao Q, Zhu H, Dong L, Shi W, Chen R, Song Z, et al. Integrated proteogenomic characterization of HBV-related hepatocellular carcinoma. Cell. 2019; 179: 561-577.
31. Dueland S, Guren TK, Hagness M, Glimelius B, Line PD, Pfeiffer P, et al. Chemotherapy or liver transplantation for nonresectable liver metastases from colorectal cancer? Ann Surg. 2015; 261: 956-960.
32. Mendiratta V, Limkemann AJ. RAPID progress: Living donor liver transplantation for unresectable colorectal liver metastases. Liver Transpl. 2026; 32: 645-646.
33. Yilmaz S. Liver transplantation for colorectal liver metastases. J Inonu Liver Transpl Inst. 2025; 3: 105-110.
34. Ritchie ME, Phipson B, Wu D, Hu Y, Law CW, Shi W, et al. limma powers differential expression analyses for RNA-sequencing and microarray studies. Nucleic Acids Res. 2015; 43: e47.
35. Clough E, Barrett T, Wilhite SE, Ledoux P, Evangelista C, Kim IF, et al. NCBI GEO: Archive for gene expression and epigenomics data sets: 23-year update. Nucleic Acids Res. 2024; 52: D138-D144.

36. Benjamini Y, Hochberg Y. Controlling the false discovery rate: A practical and powerful approach to multiple testing. J R Stat Soc Ser B Methodol. 1995; 57: 289-300.
37. Gentleman RC, Carey VJ, Bates DM, Bolstad B, Dettling M, Dudoit S, et al. Bioconductor: Open software development for computational biology and bioinformatics. Genome Biol. 2004; 5: R80.
38. Kuleshov MV, Jones MR, Rouillard AD, Fernandez NF, Duan Q, Wang Z, et al. Enrichr: A comprehensive gene set enrichment analysis web server 2016 update. Nucleic Acids Res. 2016; 44: W90-W97.
39. Kanehisa M, Goto S. KEGG: Kyoto encyclopedia of genes and genomes. Nucleic Acids Res. 2000; 28: 27-30.
40. Warde-Farley D, Donaldson SL, Comes O, Zuberi K, Badrawi R, Chao P, et al. The GeneMANIA prediction server: Biological network integration for gene prioritization and predicting gene function. Nucleic Acids Res. 2010; 38: W214-W220.
41. Mostafavi S, Ray D, Warde-Farley D, Grouios C, Morris Q. GeneMANIA: A real-time multiple association network integration algorithm for predicting gene function. Genome Biol. 2008; 9: S4.
42. Li T, Fan J, Wang B, Traugh N, Chen Q, Liu JS, et al. TIMER: A web server for comprehensive analysis of tumor-infiltrating immune cells. Cancer Res. 2017; 77: e108-e110.
43. Li T, Fu J, Zeng Z, Cohen D, Li J, Chen Q, et al. TIMER2.0 for analysis of tumor-infiltrating immune cells. Nucleic Acids Res. 2020; 48: W509-W514.
44. Cui H, Zhao G, Lu Y, Zuo S, Duan D, Luo X, et al. TIMER3: An enhanced resource for tumor immune analysis. Nucleic Acids Res. 2025; 53: W534-W541.
45. Liu Z, Guo F, Wang Y, Li C, Zhang X, Li H, et al. BATMAN-TCM: A bioinformatics analysis tool for molecular mechanism of traditional Chinese medicine. Sci Rep. 2016; 6: 21146.
46. Kong X, Liu C, Zhang Z, Cheng M, Mei Z, Li X, et al. BATMAN-TCM 2.0: An enhanced integrative database for known and predicted interactions between traditional Chinese medicine ingredients and target proteins. Nucleic Acids Res. 2024; 52: D1110-D1120.
47. Zhou Y, Yu L, Huang P, Zhao X, He R, Cui Y, et al. Identification of afatinib-associated ADH1B and potential small-molecule drugs targeting ADH1B for hepatocellular carcinoma. Front Pharmacol. 2023; 14: 1166454.
48. Seol JE, Kim J, Lee BH, Hwang DY, Jeong J, Lee HJ, et al. Folate, alcohol, ADH1B and ALDH2 and colorectal cancer risk. Public Health Nutr. 2020; 24: 677-684.
49. Liu Y, Yang J, Han W, Gu T, Yao L, Wang Y, et al. Identification and validation of metastasis-related gene ZG16 in the prognosis and progression in colorectal cancer. Front Oncol. 2024; 14: 1409329.
50. Meng H, Li W, Boardman LA, Wang L. Loss of ZG16 is associated with molecular and clinicopathological phenotypes of colorectal cancer. BMC Cancer. 2018; 18: 433.
51. Abenavoli L, Scarlata GG, Paravati MR, Boccuto L, Luzza F, Scarpellini E. Gut microbiota and liver transplantation: Immune mechanisms behind the rejection. Biomedicines. 2023; 11: 1792.
52. Don BR, Kaysen G. Serum albumin: Relationship to inflammation and nutrition. Semin Dial. 2004; 17: 432-437.
53. Wang F, Li P, Li FS. Prognostic role of C-reactive protein to albumin ratio in colorectal cancer: A meta analysis. Medicine. 2019; 98: e16064.

54. Al-Shaiba R, McMillan DC, Angerson WJ, Leen E, McArdle CS, Horgan P. The relationship between hypoalbuminaemia, tumour volume and the systemic inflammatory response in patients with colorectal liver metastases. Br J Cancer. 2004; 91: 205-207.
55. Kim KS, Kwon HM, Kim JH, Yang JW, Jun IG, Song JG, et al. C-reactive protein-to-albumin ratio is a predictor of 1-year mortality following liver transplantation. Anesth Pain Med. 2022; 17: 420-428.
56. Zhang B, Sun H, Lou L, Zhuang J, Liu G, Sun W, et al. Construction and validation of a predictive model for preoperative frailty risk in liver transplant recipients. 2024. doi: 10.21203/rs.3.rs-3890299/v1.
57. Trivedi PJ, Adams DH. Gut-liver immunity. J Hepatol. 2016; 64: 1187-1189.
58. Nicolini A, Ferrari P. Involvement of tumor immune microenvironment metabolic reprogramming in colorectal cancer progression, immune escape, and response to immunotherapy. Front Immunol. 2024; 15: 1353787.
59. Chen X, Ma Z, Yi Z, Wu E, Shang Z, Tuo B, et al. The effects of metabolism on the immune microenvironment in colorectal cancer. Cell Death Discov. 2024; 10: 118.
60. Caini P, Carloni V. Metabolism and immune suppressive response in liver cancer. Biomedicines. 2025; 13: 1461.
61. Lin J, Rao D, Zhang M, Gao Q. Metabolic reprogramming in the tumor microenvironment of liver cancer. J Hematol Oncol. 2024; 17: 6.
62. Gholamalizadeh M, Behrad Nasab M, Ahmadzadeh M, Doaei S, Jonoush M, Shekari S, et al. The association among calorie, macronutrient, and micronutrient intake with colorectal cancer: A case-control study. Food Sci Nutr. 2022; 10: 1527-1536.
63. Mannisto S, Yaun SS, Hunter DJ, Spiegelman D, Adami HO, Albanes D, et al. Dietary carotenoids and risk of colorectal cancer in a pooled analysis of 11 cohort studies. Am J Epidemiol. 2007; 165: 246-255.
64. Druesne-Pecollo N, Latino-Martel P, Norat T, Barrandon E, Bertrais S, Galan P, et al. Beta-carotene supplementation and cancer risk: A systematic review and metaanalysis of randomized controlled trials. Int J Cancer. 2010; 127: 172-184.
65. Natale A, D'Angelo A, Bidoli E, Toffolutti F, Giacosa A, Augustin LSA, et al. Intake of total and selected carotenoids and colorectal cancer risk: An Italian case-control study. Eur J Clin Nutr. 2025; 79: 1154-1159.
66. Chung J, Kang J, Kim SH, Jung MK, Kim DH, Song HJ, et al. Dietary β-carotene, vitamin A, and retinol intake and prevalence of colorectal adenoma: A cross-sectional study and meta-analysis. Gut Liver. 2025; 19: 845-859.
67. Lin WT, Huang CC, Lin TJ, Chen JR, Shieh MJ, Peng HC, et al. Effects of beta-carotene on antioxidant status in rats with chronic alcohol consumption. Cell Biochem Funct. 2009; 27: 344-350.
68. van Duijnhoven FJ, Bueno-De-Mesquita HB, Ferrari P, Jenab M, Boshuizen HC, Ros MM, et al. Fruit, vegetables, and colorectal cancer risk: The European prospective investigation into cancer and nutrition. Am J Clin Nutr. 2009; 89: 1441-1452.
69. Steck-Scott S, Forman MR, Sowell A, Borkowf CB, Albert PS, Slattery M, et al. Carotenoids, vitamin A and risk of adenomatous polyp recurrence in the polyp prevention trial. Int J Cancer. 2004; 112: 295-305.

70. Buhrmann C, Shayan P, Popper B, Goel A, Shakibaei M. Sirt1 is required for resveratrol-mediated chemopreventive effects in colorectal cancer cells. Nutrients. 2016; 8: 145.
71. Moutabian H, Majdaeen M, Ghahramani-Asl R, Yadollahi M, Gharepapagh E, Ataei G, et al. A systematic review of the therapeutic effects of resveratrol in combination with 5-fluorouracil during colorectal cancer treatment: With a special focus on the oxidant, apoptotic, and anti-inflammatory activities. Cancer Cell Int. 2022; 22: 142.
72. Schaafsma E, Hsieh TC, Doonan BB, Pinto JT, Wu JM. Anticancer activities of resveratrol in colorectal cancer. Biol Med. 2016; 8: 1000317.
73. Ji Q, Liu X, Han Z, Zhou L, Sui H, Yan L, et al. Resveratrol suppresses epithelial-to-mesenchymal transition in colorectal cancer through TGF-beta1/Smads signaling pathway mediated Snail/E-cadherin expression. BMC Cancer. 2015; 15: 97.
74. Tu KX, Ou QJ, Lin FT, Zhao YT, Zhou RH, Zhou RL, et al. Higher intake of resveratrol is associated with a lower risk of colorectal cancer: A large-scale case-control study. Phytother Res. 2025; 39: 2776-2789.
75. Totonchi H, Mokarram P, Karima S, Rezaei R, Dastghaib S, Koohpeyma F, et al. Resveratrol promotes liver cell survival in mice liver-induced ischemia-reperfusion through unfolded protein response: A possible approach in liver transplantation. BMC Pharmacol Toxicol. 2022; 23: 74.
76. Faghihzadeh F, Hekmatdoost A, Adibi P. Resveratrol and liver: A systematic review. J Res Med Sci. 2015; 20: 797-810.
77. Li L, Ahmed B, Mehta K, Kurzrock R. Liposomal curcumin with and without oxaliplatin: Effects on cell growth, apoptosis, and angiogenesis in colorectal cancer. Mol Cancer Ther. 2007; 6: 1276-1282.
78. Ge S, Sun X, Sang L, Zhang M, Yan X, Ju Q, et al. Curcumin inhibits malignant behavior of colorectal cancer cells by regulating M2 polarization of tumor-associated macrophages and metastasis associated in colon cancer 1 (MACC1) expression. Chem Biol Drug Des. 2023; 102: 1202-1212.
79. Patel BB, Sengupta R, Qazi S, Vachhani H, Yu Y, Rishi AK, et al. Curcumin enhances the effects of 5-fluorouracil and oxaliplatin in mediating growth inhibition of colon cancer cells by modulating EGFR and IGF-1R. Int J Cancer. 2008; 122: 267-273.
80. Howells LM, Mitra A, Manson MM. Comparison of oxaliplatin- and curcumin-mediated antiproliferative effects in colorectal cell lines. Int J Cancer. 2007; 121: 175-183.
81. Saidi SA, Meurisse N, Jochmans I, Heedfeld V, Wylin T, Parkkinen J, et al. Hepatocellular uptake of cyclodextrin-complexed curcumin during liver preservation: A feasibility study. Biopharm Drug Dispos. 2018; 39: 18-29.
82. Chen C, Johnston TD, Wu G, Ranjan D. Curcumin has potent liver preservation properties in an isolated perfusion model. Transplantation. 2006; 82: 931-937.
83. Thuillier R, Allain G, Giraud S, Saintyves T, Delpech PO, Couturier P, et al. Cyclodextrin curcumin formulation improves outcome in a preclinical pig model of marginal kidney transplantation. Am J Transplant. 2014; 14: 1073-1083.
84. Alfonso-Moreno V, Lopez-Serrano A, Moreno-Osset E. Chemoprevention of polyp recurrence with curcumin followed by silibinin in a case of multiple colorectal adenomas. Rev Esp Enferm Dig. 2017; 109: 875.

85. Chen MB, Wu XY, Tao GQ, Liu CY, Chen J, Wang LQ, et al. Perifosine sensitizes curcumin-induced anti-colorectal cancer effects by targeting multiple signaling pathways both *in vivo* and *in vitro*. Int J Cancer. 2012; 131: 2487-2498.
86. Cen L, Hutzen B, Ball S, DeAngelis S, Chen CL, Fuchs JR, et al. New structural analogues of curcumin exhibit potent growth suppressive activity in human colorectal carcinoma cells. BMC Cancer. 2009; 9: 99.
87. Woo JH, Kim YH, Choi YJ, Kim DG, Lee KS, Bae JH, et al. Molecular mechanisms of curcumin-induced cytotoxicity: Induction of apoptosis through generation of reactive oxygen species, down-regulation of Bcl-XL and IAP, the release of cytochrome c and inhibition of Akt. Carcinogenesis. 2003; 24: 1199-1208.
88. Andrews PM, Cooper M, Verbesey J, Ghasemian S, Rogalsky D, Moody P, et al. Mannitol infusion within 15 min of cross-clamp improves living donor kidney preservation. Transplantation. 2014; 98: 893-897.
89. DeMaria Jr S, Bachner EM, Mroz V, Gamboa S, Ouyang Y, Egorova NN, et al. The efficacy of mannitol in attenuating postreperfusion syndrome in orthotopic liver transplantation: A retrospective cohort study. J Clin Med. 2025; 14: 1897.
90. Emara MM, Diab DG, Yassen AM, Abo-Zeid MA. Mannitol for prevention of acute kidney injury after liver transplantation: A randomized controlled trial. BMC Anesthesiol. 2022; 22: 393.